Giant magnetoresistance of Fe_3O_4-polymethylmethacrylate nanocomposite aligned fibers via electrospinning

Cite as: J. Appl. Phys. **101**, 114317 (2007); https://doi.org/10.1063/1.2745197
Submitted: 23 February 2007 . Accepted: 18 April 2007 . Published Online: 13 June 2007

V. S. Pavan Kumar, V. Jagadeesh Babu, G. K. Raghuraman, R. Dhamodharan, and T. S. Natarajan

Giant magnetoresistance of Fe_3O_4-polymethylmethacrylate nanocomposite aligned fibers via electrospinning

V. S. Pavan Kumar and V. Jagadeesh Babu
Department of Physics, Indian Institute of Technology Madras, Chennai 600036, India

G. K. Raghuraman and R. Dhamodharan
Department of Chemistry, Indian Institute of Technology Madras, Chennai 600036, India

T. S. Natarajan[a)]
Department of Physics, Indian Institute of Technology Madras, Chennai 600036, India

(Received 23 February 2007; accepted 18 April 2007; published online 13 June 2007)

This paper describes the results of investigations on giant negative magnetoresistance (GMR) in nanocomposite aligned fibers prepared using electrospinning. The nanocomposite contains polymethylmethacrylate (PMMA) matrix and the nanoparticles of polymer (PMMA) grafted magnetite, Fe_3O_4 (PGM). Even for the low magnetic field (1 T) a GMR of about 50% was observed for low loading (5 wt %) of PGM at room temperature. The fibers were characterized using scanning electron microscope and high resolution transmission electron microscope. X-ray diffraction (XRD) patterns were recorded for clean PMMA fibers, PMMA granules, and PGM nanoparticles. The dc conductivity was calculated from the *I-V* characteristics for the fibers at room temperature. © *2007 American Institute of Physics*. [DOI: 10.1063/1.2745197]

INTRODUCTION

Polymer nanocomposites with magnetic fillers are now being extensively studied because of their high application potential.[1] These materials, containing conducting filler particles at concentrations above the percolation threshold, should behave as conductor and exhibit certain magnetic-field-sensitive properties, such as Hall effect or magnetoresistance (MR). These effects not only allow them to be classified as smart materials but also help in establishing the mechanism of conduction in such complex disordered systems. Recent wave of interest in magnetic nanocomposites has arisen because of their extensive applications in magnetic shielding, rewritable magnetic memories, etc. Research activities have been focusing on the MR of different forms including single crystals, epitaxial and polycrystalline films, fibers, powders, and tunneling junctions involving Fe_3O_4 as electrodes.[2–6] Among these various forms of nanocomposites, fibers of diameters in the nanometer range are attractive as they have high surface area to volume ratio. In order to prepare polymer nanocomposite fibers, there are different techniques available.[7,8] Electrospinning is proposed as an easy one step nonmechanical process to fabricate one-dimensional polymer fibers/ribbons.[9] There has been keen interest in the half metallic magnetite, Fe_3O_4, because of its highly spin polarized nature ($\sim$100%) and high Curie temperature ($T_C \sim 840$ K) which are desirable properties in spin electronic devices.[10,11] This paper reports on the investigations done on the electrospun fibers of polymethymethacrylate (PMMA) matrix filled with ferromagnetic nanoparticles of polymer grafted magnetite (PGM). This type of nanocomposite was prepared to functionalize the existing polymer to enhance the conductivity of clean polymer and to study the conductive nature of the nanocomposite in magnetic field. The significance of this nanocomposite system is due to the modifications the filler particles were subjected to before electrospinning in order to obtain good dispersion in both high and low concentrations of PMMA matrix. Here PMMA brushes were grafted on the surface of the Fe_3O_4 nanoparticles through chemical means, otherwise the metal nanoparticles tend to agglomerate and form clusters. Good dispersion could be achieved with the PMMA brushes in the solution. The PMMA-PGM nanocomposite system were electrospun in the form of aligned electrospun fibers and were characterized by scanning electron microscopy (SEM) micrograms, x-ray diffraction (XRD), dc conductivity, and giant MR (GMR) measurements at room temperature. The results of these investigations are discussed in detail.

EXPERIMENT

PMMA granules were obtained from Union Carbide. Tetrahydrofuran (THF) was obtained from Sisco Research Laboratories, India. All the chemicals were used as received. PGM nanoparticles were synthesized using analytical grade reagents, as described elsewhere.[12] Initially, PGM was grinded well and subjected to sonication (ultrasonic agitation) for 2 h in THF to disperse the nanoparticles. This solution was filtered through a 0.2 μm polytetrafluroethylene (PTFE) (Whatman, USA) syringe filter to avoid micron sized agglomerated clusters if any. This filtrate was dried and contained PGM nanoparticles in the size $\leqslant$0.2 μm. These particles were used to prepare the nanocomposite.

Required amounts of PGM nanoparticles were dispersed in THF by sonication for 1 h. Then preweighed PMMA was added in order to prepare a composite with 5 wt % of magnetite and 15 wt % of PMMA solution in THF. This solution was subjected to overhead stirring for 12 h. During stirring

[a)]Electronic mail: tsn@physics.iitm.ac.in

the sample vial was kept in ice at 0 °C to avoid the evaporation of the THF. The PGM showed good stability in dispersion not only in organic solvents but also in the polymer composite solution. This solution was utilized for electrospinning using an apparatus described elsewhere in detail.[13] The solution was subjected to sonication for 1 h prior to electrospinning. The parameters for electrospinning were optimized and are as follows: the distance between the electrodes was 65 mm, the diameter of the needle was 0.56 mm, the speed of rotation of the collecting screen was 1500 rpm (equivalent to a linear velocity of 190 m/s at the drum surface), and the flow rate of the solution was ~0.7 μl/h.

The surface morphology of the fibers was characterized using SEM from JEOL JSM 840A. Prior to the examination, electrospun fiber mat was sputter coated with a 50 Å layer of gold. The recorded images were imported into UTHSCSA IMAGE TOOL 3.0 software for determining the diameter and orientation of the fibers (relative to the direction of rotation of the substrate). The fibers were also collected on copper grid for recording the HRTEM images from JEOL 3010 transmission electron microscope with a ultra high resolution (UHR) pole piece.

Structural characterization was done by obtaining the XRD pattern of the fiber mat in order to detect the crystalline nature of the fibers, if any, using x-ray diffractometer (X'Pert PRO PANalytical). This was performed on PMMA granules, clear PMMA fibers, and PGM nanoparticles individually. The fibers of pure PMMA were collected for about 4 h on an aluminum foil in order to obtain self-standing nonwoven mat. This mat was placed on a Si single crystal and the XRD data were recorded. In the case of nanoparticles and clean PMMA granules, they were sprinkled on a clean glass slide on which a thin layer of silicone grease was applied. The wavelength used was 1.5418 Å, step scanning with step size of 0.01°.

For electrical characterizations, electrospun fibers were collected on a set of silver (Ag) electrodes thermally evaporated on a clean glass slide. The separation of the electrodes was nearly 1 mm and was fairly uniform. After forming the fibers, the Ag electrodes were deposited again on top using the same mask as before to achieve better electrical contact as well as to prevent the fibers from dislodging from the substrate when the magnetic field is applied.

The dc resistance of the fibers was obtained by using a homemade variable voltage source and Keithley 480 picoammeter. The average dc conductivity of the fibers was estimated by considering the number of fibers, average width, and the distance between the electrodes.

The GMR measurements were performed using Keithley 617 programmable electrometer in resistance mode directly to measure the change in the resistance at room temperature with different applied magnetic fields (0–1 T). The fibers were held parallel to the magnetic field [electron spin resonance (ESR) electromagnets belonging to ESR apparatus Varian E-112].

RESULTS AND DISCUSSION

Aligned electrospun fibers of PMMA-PGM nanocomposite were obtained by optimizing the parameters (collection speed and spinning rate). The fibers were free of defects such as beads[14] or lumps. This indicates that there are no big cluster of PGM nanoparticles at micron level. It is observed from the SEM pictures in Fig. 1(a) that the fibers are not of circular cross section but in the form of ribbons with the ratio of thickness to width of around 0.39, and lengths are in the order of several millimeters. The inset of Fig. 1(a) shows a twisted ribbon. The hollow fibers formed collapsed as the solvent evaporated and thus resulted in a ribbonlike structure. The impact and the interaction of the charged fiber with the surface of the substrate, namely, the aluminum foil also affected the fiber morphology.[15,16] In Fig. 1(b) we observe that the surface of the ribbon is not smooth.[17] From the distribution graph in Fig. 2, we see that the fibers have wide range of diameters with a mean at 7 μm. The fibers are also aligned in the direction of the rotation of the collecting drum, as seen qualitatively from the SEM pictures. However, in

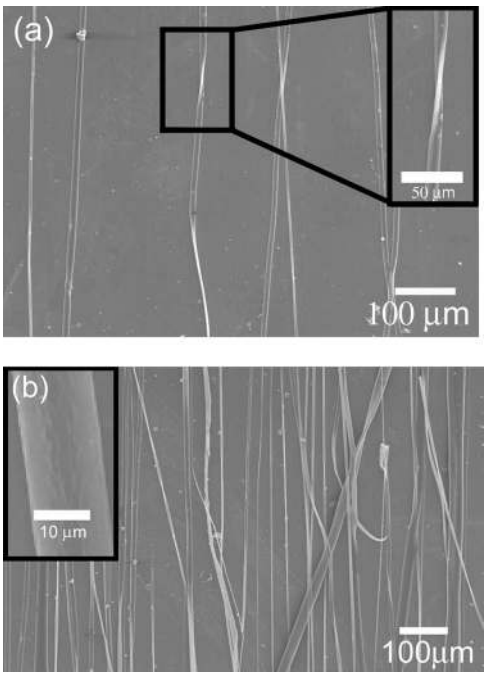

FIG. 1. SEM images of electrospun fibers obtained for two different times: (a) for 30 s and (b) for 150 s. The ribbonlike structure is seen clearly. The inset of (a) shows a twisted ribbon of nanocomposite, and that of (b) shows the surface features of the fiber at higher magnification.

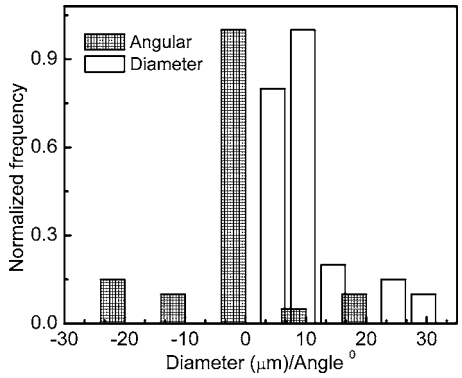

FIG. 2. Representation of the angular and diameter distributions against normalized frequency.

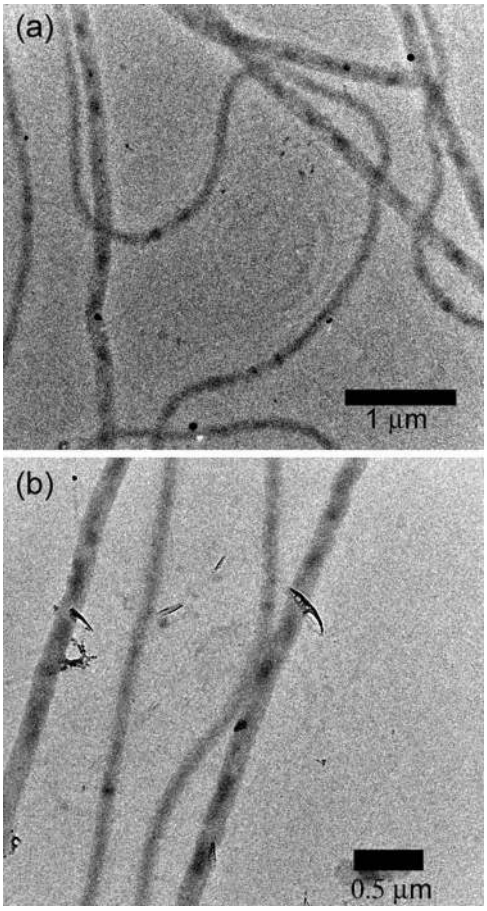

FIG. 3. HRTEM images of electrospun nanocomposite fibers.

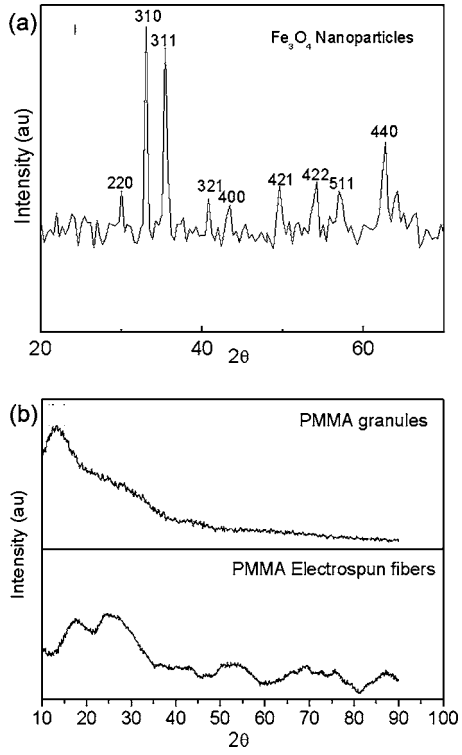

FIG. 4. XRD patterns of (a) magnetite nanoparticles, (b) clear PMMA granules, and that of ribbon mat of clear PMMA.

order to quantitatively estimate the alignment achieved, the angular distribution of the fibers is plotted in Fig. 2, where the distribution function is adopted from Fisher[18] for a periodicity of π radians, μ is the mean angle=0.17, ρ is the mean resultant length=0.19, and standard deviation σ=0.90. Since the mean angle is small, we can conclude that the alignment achieved was very good.

The embedded PGM particles can be observed in the HRTEM image in Figs. 3(a) and 3(b). The average diameter of PGM nanoparticles is around 80 nm. The average distance between two consecutive particles in the fiber is around 200 nm, but the distribution is varying from 50 to 450 nm, which shows that the particles are not in contact with each other. The XRD results are plotted between the intensity in arbitrary units and twice the Bragg angle (2θ) (see Fig. 4). The XRD patterns show that all of the nanoparticles are highly crystalline materials. The crystalline features were confirmed by the excellent matching of the diffraction peaks with that for standard spectrum. The mismatch in the intensity of the peaks with reference pattern is because of preferred orientation; i.e., particles may be oriented with respect to the x-ray beam in such a way that the contribution from a particular plane was enhanced or suppressed.[19] The mean particle diameters were also calculated from the XRD pattern according to the linewidth of the (310) plane refraction peak using Scherrer equation, $D=K\lambda/(b\cos\theta)$, which gives the thickness of the crystal perpendicular to the corresponding *hkl* values.[19] This equation uses the reference peak width at twice Bragg angle θ (15.5°), where λ is the x-ray wavelength (1.5418 Å), b is the width of the XRD peak at half-height, and K is the shape factor, about 0.9 for magnetite.[19] The result was ~19 nm for magnetite nanoparticles.

Figure 4(b) shows the results of XRD measurements on PMMA granules and electrospun fibers of PMMA. While the peaks of the magnetite particles could be well assigned we did not observe any peak in the case of PMMA granules. This shows that the polymer is mostly amorphous in nature. However, the XRD measurements on the fibers show several broad peaks and the corresponding θ values match the International Crystal Diffraction Data[25] of PMMA. This means that the crystallinity of the polymer increases on electrospinning. This is similar to the earlier reports on polycaprolactone nanofibers where improvement in crystallinity was observed due to electrospinning. It is known that when the polymer solution is forced through a nozzle under high electric field they get oriented in the direction of the fiber axis which can lead to better ordering of the molecules and consequent increase in their crystallinity when the polymer solidifies quickly during its travel toward the counterelectrode.[20–22]

The *I-V* characteristics of an array of fibers recorded at room temperature is shown in Fig. 5(a). The plot is linear showing a simple Ohmic behavior. The dc conductivity was evaluated using the average diameter of the fibers estimated using the IMAGE TOOL software from the SEM pictures. The value was found to be $\sim 12\times 10^{-9}$ S/m. The enhancement in the conductivity is by approximately four orders of magnitude compared to the pure PMMA.[23] It appears that the concentration of the magnetite in the composite is either below or in the region of percolation threshold and hence there is

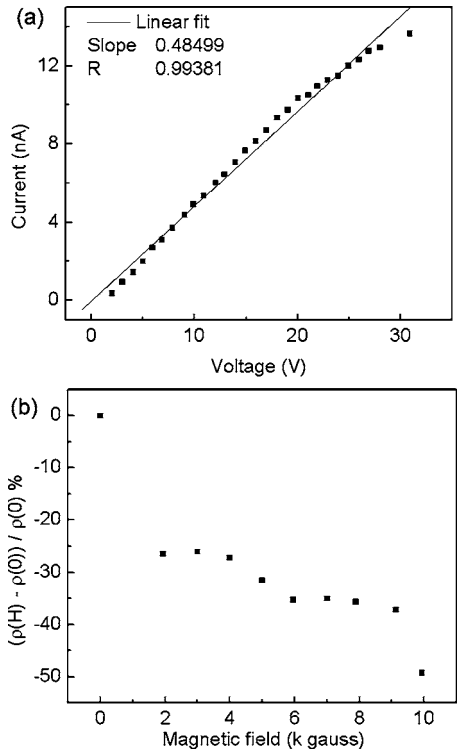

FIG. 5. (a) Current-voltage characteristics and (b) GMR behavior of the magnetite-PMMA nanocomposite fibers at room temperature.

only a small change in the conductivity. It has been observed earlier that the polystyrene-magnetite composite showed very low resistance and the enhancement was attributed to interparticle tunneling.[24] Here, in this case of PMMA we also find that the particles which can be clearly resolved using HRTEM are about 200 nm apart on an average. There could even be smaller particles which could not be observed with HRTEM. Hence the conduction mechanism in this case could also be due to interparticle tunneling. Due to the layer of polymer present in between the PGM particles, the surfaces of the PGM particles are free from oxygen which is believed to alter the half-metallic state at the surface. In this case it could not be categorically resolved since the temperature dependent conductivity data are not available.

The GMR behavior is shown in Fig. 5(b) where the change in the resistivity of the fibers is plotted against the applied magnetic field. We observe a sharp fall initially up to 2 kG field and then a gradual fall from 2 to 9 kG finally; around 1 T it reaches 50% mark showing a negative magnetoresistance behavior. This is significant even for such small variation of magnetic field by about 1 T. Initially, the molecules are in antiferromagnetic alignment and the electron faces high resistance and after the application of the field, the particles align ferromagnetically and hence resistance is low. The drastic enhancement of the GMR is attributed to the fact that the polymer is an excellent barrier material and more importantly prevents the oxidation of the surface of Fe_3O_4. Results clearly suggest that there is a high degree of spin polarization at room temperature for half-metallic Fe_3O_4 in this nanocomposite.[24]

CONCLUSION

Electrospun fibers of PMMA-PGM nanocomposite were characterized through SEM and found to have a ribbonlike structure. From HRTEM images the average diameter of the particles is around 80 nm and the average interparticle distance is about 200 nm. Since there is a certain distance between the PGM nanoparticles, the electrical conduction may be due to tunneling phenomena. The x-ray diffraction patterns show an increase in the crystallanity of PMMA fibers in comparison to the granules. The *I-V* characteristics of the fibers show a normal Ohmic behavior with the conductivity increase by nearly four orders of magnitude. The magnetoresistance measurements on the fibers in the range of fields from 0 to 1 T show a drastic fall initially and then a gradual decrease. The overall resistance variation for a change in magnetic field from 0 to 1 T is nearly 50%, which is indeed significant.

[1] N. Crainic and A. T. Marques, Key Eng. Mater. **230–232**, 656 (2002).
[2] V. V. Gridin, G. R. Hearne, and J. M. Honig, Phys. Rev. B **53**, 15518 (1996).
[3] W. Eerenstein, T. T. M. Palstra, S. S. Saxena, and T. Hibma, Phys. Rev. Lett. **88**, 247204 (2002).
[4] W. Eerenstein, T. T. M. Palstra, T. Hibma, and S. Celotto, Phys. Rev. B **66**, 20110 (2002).
[5] M. D. Coey, A. E. Berkowitz, L. Balcells, F. F. Putris, and F. T. Parker, Appl. Phys. Lett. **72**, 734 (1998).
[6] L. Peng, T. Asai, N. Nozawa, T. Hihara, and K. Sumiyama, Appl. Phys. Lett. **81**, 4598 (2002).
[7] T. Ondarcuhu and C. Joachim, Europhys. Lett. **42**, 215 (1998).
[8] H. Li, Y. Ke, and Y. Hu, J. Appl. Polym. Sci. **99**, 1018 (2006).
[9] A. Formhals, U.S. Patent No. 1,975,504 (October 2, 1934).
[10] A. M. Bratkovsky, Phys. Rev. B **56**, 2344 (1997).
[11] A. M. Bratkovsky, Appl. Phys. Lett. **72**, 2334 (1998).
[12] G. K. Raghuraman and R. Dhamodharan, J. Nanosci. Nanotechnol. **6**, 2018 (2006).
[13] B. Sundaray, V. Subramanian, T. S. Natarajan, Rong-Zheng Xiang, Chia-Cheng Chang, and Wun-Shain Fann, Appl. Phys. Lett. **84**, 1222 (2004).
[14] C. Hsu and S. Shivkumar, J. Mater. Sci. **39**, 3003 (2004).
[15] V. Bergeron, D. Bonn, J. Y. Martin, and L. Vovelle, Nature (London) **405**, 772 (2000).
[16] J. T. McCann, J. I. L. Chen, D. Li, Z.-G. Ye, and Y. Xia, Chem. Phys. Lett. **424**, 162 (2006).
[17] M. Bognitzki, T. Frese, M. Steinhart, A. Greiner, J. H. Wendorff, A. Schaper, and M. Hellwig, Polym. Eng. Sci. **41**, 982 (2001).
[18] N. I. Fisher, *Statistical Analysis of Circular Data* (Cambridge University Press, New York, 1993).
[19] U. Schertmann and R. M. Cornell, *Iron Oxides in the Laboratory: Preparation and Characterization* (VCH, Weinheim, 1991).
[20] X. M. Moa, C. Y. Xub, M. Kotakib, and S. Ramakrishna, Biomaterials **25**, 1883 (2004).
[21] K. H. Lee, H. Y. Kim, Y. M. La, D. R. Lee, and N. H. Sung, J. Polym. Sci., Part B: Polym. Phys. **40**, 2259 (2002).
[22] D. H. Reneker, W. Kataphinan, A. Theron, E. Zussman, and A. L. Yarin, Polymer **43**, 6785 (2002).
[23] D. Charles, R. C. Weast, and S. M. Selby, *Handbook of Chemistry and Physics* (Chemical Rubber Company, Cleveland, OH, 1960).
[24] W. Wang, M. Yu, Y. Chen, and J. Tang, J. Appl. Phys. **99**, 08J108 (2006).
[25] H. Okamura, J. Polym. Sci. **46**, 539 (1960); JCPDS Card No. 13-0835.